Li Y, et al. Supplemental Fig. 1

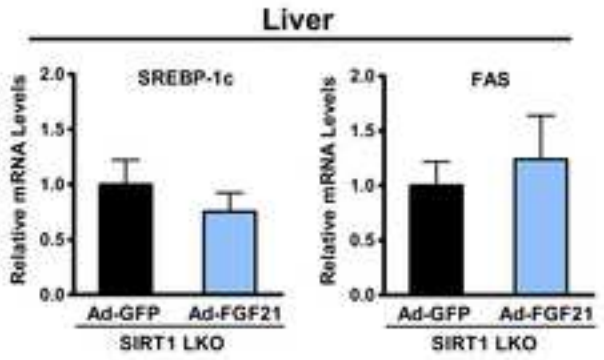

Fig. S1. Hepatic expression of SREBP-1c and FAS in fasted SIRT1 LKO mice is not affected by hepatic overexpression of FGF21. Adenoviruses (5×10^9 pfu) encoding either FGF21 or control GFP were delivered into 8- to 10-month-old mice (n = 4-7) via tail vein injection. The animals were sacrificed in a 24-h fast state after 2 weeks of injection.

Li Y, et al. **Supplemental Materials and Methods**

Reagents and Antibodies—The Quantikine Mouse FGF21 ELISA kit (Cat# MF2100) was from R&D Systems (Minneapolis, MN). The β-Hydroxybutyrate LiquiColor Test kit (Cat# 2440-058) was from Stanbio Laboratory. The Dual-Luciferase Reporter Assay kit was purchased from Promega (Madison, WI). Anti-FGF21 antibody (monoclonal; clone# 84-E12; raised against human FGF-21 protein) was described previously[1]. Rabbit polyclonal SIRT1 antibody (Cat# 07-131) was from Millipore (Billerica, MA). SIRT1 antibody *(*H-300*,* Cat# sc-15404) as well as horseradish peroxidase-conjugated anti-mouse and anti-rabbit secondary antibodies were obtained from Santa Cruz Biotechnology Inc. (Santa Cruz, CA).

Liver-specific SIRT1 Knockout (SIRT1 LKO) Mice—SIRT1 LKO mice were generated by crossing albumin-Cre recombinase transgenic mice with floxed $SIRT1^{\Delta ex4}$ mice containing the deleted SIRT1 exon 4, which encodes 51 amino acids of the conserved SIRT1 catalytic domain [2, 3]. SIRT1 LKO mice of the C57BL/6 genetic background were previously described [3]. These mice were genotyped with the following primers: 5' CCCCATTAAAGCAGTATGTG 3' (F) and 5' CATGTAATCTCAACCTTGAG 3' (R) for the floxed *SIRT1* gene; 5' GTTAATGATCTACAGTTATTGG 3' (F), 5' CGCATAACCAGTGAAACAGCATTGC 3' (R) for the *Alb-Cre* gene. SIRT1 LKO mice ($Cre^{+/-}/SIRT1^{flox/flox}$) and their littermates ($Cre^{-/-}/SIRT1^{flox/flox}$) were used for experiments. Mice were maintained on a 12-h light-dark cycle in a temperature-controlled barrier facility with free access to water and food. These procedures were approved by the Boston University Medical Center Institutional Animal Care and Use Committee.

Animal Fasting and Refeeding Experiments—SIRT1 LKO mice and WT littermates were divided into three groups: fed, fasted, and refed, as described previously[4, 5]. The fed group was placed on a normal chow diet; the fasted group was fasted for 24 h; and the refed group was fasted for 24 h and additionally refed for 6 h prior to the end of experiments. When mice were sacrificed under isoflurane anesthesia, tissues were rapidly taken, freshly frozen in liquid nitrogen, and stored at -80°C until needed for biochemical analysis.

Gene Expression Array—Gene expression chip array was performed using the Fluidigm BioMark system. Predesigned TaqMan® probes and primers were obtained from Applied Biosystems (ABI, Foster City, CA, USA).

Quantitative Real-Time-PCR—First-strand cDNA was generated by reverse transcription using total RNA. Real-time PCR was performed using the Applied Biosystems StepOnePlus Real-Time PCR System (Applied Biosystems, Foster City, CA) and the SYBR green kit, as described previously[5-7]. Primers were designed using Primer3 (Table S1). The mRNA abundance of tested genes is determined by qRT-PCR, normalized to that of β-actin, and expressed as relative mRNA levels.

Immunoblotting Analysis—Mouse liver tissues or cultured cells were lysed at 4°C in lysis buffer containing 20 mM Tris-HCl, pH 8.0, 1% (v/v) Nonidet P-40, 150 mM NaCl, 1 mM EDTA, 1 mM EGTA, 1 mM sodium orthovanadate, 25 mM β-glycerolphosphate, 1 mM dithiothreitol, 1 mM phenylmethylsulfonyl fluoride, 2 μg/ml aprotinin, 2 μg/ml leupeptin, and 1 μg/ml pepstatin, as described previously[5, 6, 8-10]. The protein levels of SIRT1 or FGF21 are visualized by immunoblots and normalized to β-actin levels.

Measurement of Plasma FGF21 Levels—Plasma FGF21 levels were measured using the Quantikine Mouse FGF21 ELISA kit (R&D Systems) with a minimum detectable dose of 3.81 pg/ml, according to the manufacturer's instructions. Mouse plasma samples (50 μl) were mixed with 50 μl of Assay Diluent in a 96-well plate, and the reactions were incubated on a plate shaker at room temperature for 2 h. After washing the plate 5 times, 100 μl of mouse FGF-21 conjugate were added to each well, and the

reactions were incubated at room temperature for 2 h. After washing the plate 5 times, 100 µl of substrate solution were added into each well, followed by plate incubation at room temperature for 30 min in the dark. Once 100 µl of stop reaction solution were added to each well, the optical density at 450 nM was measured in a microplate reader Infinite® M1000 (TECAN, Switzerland). Plasma FGF21 concentrations were calculated according to the standard curve.

Measurement of Hepatic Protein Concentrations of FGF21—Liver tissue was homogenized in Lysing Matrix D bead tubes (MP Biomedicals #6913-500) in 0.4ml ice-cold RIPA buffer (Thermo Scientific #89901) with 1X Halt Protease and Phosphatase Inhibitor Cocktail (Thermo Scientific #1861281) at 4^{o}C. Homogenates were solubilized by mixing in cold room for 30 minutes and subjected to centrifugation for 10 minutes at 12,000 xg at 4^{o}C, after which the supernatant was collected and protein concentration was determined (Coomassie Plus Protein Assay Reagent, Pierce #1856210). FGF21 concentrations were then determined using ELISA (R&D systems, MF2100) and normalized to protein concentration.

Measurement of Blood Glucose, Plasma Insulin, Plasma and Hepatic Lipids—Blood glucose concentrations were determined using the AlphaTRAK Glucose Meter from Abbott Laboratories (North Chicago, IL). Mouse plasma insulin was measured with an ultrasensitive mouse insulin ELISA kit (Mercodia AB, Uppsala, Sweden) as described previously[7]. Plasma and liver triglyceride and cholesterol levels were analyzed as described previously[6, 7, 9, 11].

Liver Oil Red O Staining—When animals were sacrificed, livers were embedded in OCT and rapidly frozen on the dry. Hepatic steatosis was assessed by Oil Red-O staining in OCT-embedded samples using the Oil Red O Stain Kit from American MasterTech (Lodi, CA) according to the manufacturer's protocol. Cryosections were fixed in 60% isopropanol for 10 min, stained with 0.3% Oil Red-O in 60% isopropanol for 30 min, and subsequently washed with 60% isopropanol. Sections were counterstained with Gill's hematoxylin, washed with acetic acid solution (4%), and mounted with aqueous solution. Staining images were captured and digitalized using an Olympus UC30 digital camera attached to an Olympus BX40 microscope. Relative areas of steatosis were quantified by histomorphometry using a computerized image analysis system (ImageJ, National Institutes of Health) and expressed as percentage of area stained with Oil Red O. For each image, the individual staining pattern was generated through the use of ImageJ's color deconvolution according to previously described methods[12].

Body Composition Analysis—Body composition was determined with the nuclear magnetic resonance (NMR) system using a Body Composition Analyzer Echo 900 (Echo Medical Systems, Houston, TX) as described previously[5]. Body fat, lean mass, body fluids, and total body water were measured in live, conscious mice with *ad libitum* access to chow.

Comprehensive Metabolic Monitoring—Energy expenditure was assessed by indirect calorimetry measurements using Comprehensive Laboratory Animal Monitoring Systems (CLAMS) (Columbus Instruments, Columbus, OH) in the Metabolic Phenotyping Core at Boston University School of Medicine, as described previously[5, 13, 14]. Mice of both genotypes were individually housed, acclimatized to respiratory chambers for 24 h, and allowed free access to food and water. The data for oxygen consumption (VO_2), carbon dioxide production (VCO_2), and locomotor activity were simultaneously recorded over a 48-h period which was divided into a 24-h feed and a 24-h fast. The VO_2 and VCO_2 rates were expressed as average values measured every 18 min over a 12-h block in the light and dark cycles. The energy expenditure (kcal/kg/h) was calculated with the formula $[(3.815 + 1.232 \times VCO_2/VO_2) \times VO_2 \times 0.001]$ and normalized to lean body mass as described previously[15, 16]. Physical activity was measured on X- and Y- axes by using infrared beams to count the bean breaks in the same CLAMS cage. The values were then summed ($X_{amb} + Y_{amb}$) over 12-h intervals of the light and dark cycles, respectively.

Food Intake and Body Temperature Measurements—After one week of adaptation, food intake of each individual mouse, as measured in grams of food, was recorded daily for one week. During each 24-h period, each mouse was housed with a thin layer of bedding, and a known quantity of diet was provided. After 24 h, the remaining food was weighed. Body temperature was assessed with implanted programmable subcutaneous biocompatible microchip transponders (IPTT-300 Extended Accuracy Calibration; Bio Medic Data Systems, Seaford, DE) over the mouse's shoulder blades as instructed by the manufacturer. This procedure involved light anesthesia using isoflurane, disinfection of the back area with surgical scrub (betadine), tenting of the skin over the shoulder blade area, quick insertion of a needle delivery device containing the microchip, and depression of the plunger on the device that expelled the microchip from the delivery device. MB-10 was used to maintain sterility in the surgical environment. Body temperature was measured using a DAS-6007 Probe (Bio Medic Data Systems).

***In Vivo* Adenoviral Gene Transfer—** The adenovirus producing mouse FGF21 was generated and purified by using the Adenovirus Purification Kit (Puresyn, Malvern, PA), as described previously[5, 6, 8, 10, 11]. For the amplification and purification of high-titer recombinant adenoviruses, large-scale of HEK293A cells were infected with viral supernatant at a multiplicity of infection of approximately 10 pfu per cell. Adenovirus-mediated overexpression of FGF21 in the liver of mice was accomplished through intravenous injection. One hundred microliters of adenovirus (5×10^9 - 1×10^{10} pfu) per mouse were injected into the tail vein using a 0.1-ml syringe with a 29.5-gauge needle. Two weeks post-injection, each group of mice was sacrificed under isoflurane anesthesia.

Dual Luciferase Activity Assays— A human FGF21 promoter-driven luciferase plasmid encoding a 5'-flanking fragment of the human FGF21 (-2090/+117) promoter was described previously[5, 6].HepG2 cells in a 12-well plate were co-transfected with 0.5 μg of plasmids encoding FGF21-Luc promoter, along with 20 ng of *Renilla* luciferase plasmid pRL-SV40 (Promega) as an internal control, as described previously[5, 6]. Dual luciferase assays for *Firefly* luciferase and *Renilla* luciferase activities were performed in duplicates according to the manufacturer's protocols (Promega). Luciferase activity was measured using a Turner ED-20e Luminometer. The *Firefly* luciferase activity was normalized to the *Renilla* luciferase activity (*Firefly* luciferase/*Renilla* luciferase) and presented as relative luciferase activity.

Cell Treatments and RNA Interference—Human HepG2 cells, mouse embryonic fibroblasts (MEFs) derived from wild-type and SIRT1$^{-/-}$ mice, human embryonic kidney 293T cells (HEK293T) and human embryonic kidney 293A cells (HEK293A) were cultured, as described previously [6, 9-11, 17]. HepG2 cells were treated without or with either resveratrol (10 μM) or SRT1720 (5 μM) in serum-free DMEM for 24 h. For RNA interference, FGF21 knockdown was performed using a siRNA oligonucleotides targeting human FGF21 (GCCUUGAAGCCGGGAGUUA, Cat# J-013305-06-0005) from Dharmacon RNAi Technology, Thermo Fisher Scientific (Lafayette, CO). ON-TARGET plus Non-targeting Pool (Cat # D-001810-10-05) was used as the control siRNA oligonucleotide.

XF24 Oxygen Consumption Assays and Bioenergetics Profiles—Oxygen consumption rates (OCR) in live cells were measured using the XF24 extracellular flux analyzer from Seahorse Bioscience, as described previously [18]. HepG2 cells or MEFs were seeded in a 24-well XF24 V28 cell culture microplate (Seahorse Bioscience) at a density of 20,000 cells per well in 200 μl of DMEM supplemented with 10% FBS for 16 h in a 5% CO_2 incubator at 37 °C before the experiments. Cells were washed and incubated in 630 μl of non-buffered DMEM (without sodium carbonate) at 37°C in a non-CO_2 incubator. Triplicates per treatment were included in the experiments, and four wells evenly distributed in the microplate were used for the correction of temperature variation. During the experiments, oxygen concentration was measured for 3 min within a 7-min interval, which also included a 2-min mixing period and a 2-min waiting period. A bioenergetics profile composed of basal mitochondrial respiration, ATP turnover, H^+ leak, mitochondrial respiratory capacity, and non-mitochondrial respiration was determined by calculating the area under the curve. The OCR in basal

condition was first determined and used to calculate the basal mitochondrial respiration. After this, the ATP synthase was inhibited by oligomycin (2.5 μM), creating an accumulation of protons in the mitochondrial intermembrane space and a decrease in the electron transport chain (ETC) activity, reducing the OCR. This reduction in OCR from the basal state reflected the respiration driving ATP synthesis in the cells (ATP turnover). The remaining oxygen consumption was composed of the proton leak, which maintained a minimal ETC activity and non-mitochondrial respiration. In this situation of high proton gradient and low ETC activity, addition of a mitochondrial uncoupler, carbonyl cyanide-p-trifluoromethoxyphenylhydrazone (FCCP, 1.5 μM), allowed the ETC to resume its pumping activity by dissipating the proton gradient across the inner mitochondrial membrane. This induced an increase in the OCR, and FCCP continually dissipated the protons across the membrane, the ETC activity was challenged to its maximal capacity. The oxygen consumption rates during this phase reflected the maximal mitochondrial respiratory capacity. Furthermore, treatment with antimycin (4 μM), an inhibitor of electron transfer, completely suppressed ETC activity. As a result, the OCR dropped dramatically, and the oxygen consumed in this situation by the cells came from a non-mitochondrial respiration. Finally, the basal mitochondrial respiration was calculated by subtracting non-mitochondrial OCR in antimycin A-treated cells from the OCR in pretreated cells.

Statistical Analysis—Values are expressed as the mean ± S.E.M. Statistical significance was evaluated using an unpaired two-tailed t-test or a one-way ANOVA if there were more than two groups. Differences were considered significant at the $P<0.05$ level.

References

1. Izumiya Y, Bina HA, Ouchi N, Akasaki Y, Kharitonenkov A, Walsh K. FGF21 is an Akt-regulated myokine. Febs Letters 2008;582:3805-3810.
2. Cheng HL, Mostoslavsky R, Saito S, Manis JP, Gu Y, Patel P, Bronson R, Appella E, Alt FW, Chua KF. Developmental defects and p53 hyperacetylation in Sir2 homolog (SIRT1)-deficient mice. Proc Natl Acad Sci U S A 2003;100:10794-10799.
3. Chen D, Bruno J, Easlon E, Lin SJ, Cheng HL, Alt FW, Guarente L. Tissue-specific regulation of SIRT1 by calorie restriction. Genes & Development 2008;22:1753-1757.
4. Engelking LJ, Kuriyama H, Hammer RE, Horton JD, Brown MS, Goldstein JL, Liang G. Overexpression of Insig-1 in the livers of transgenic mice inhibits SREBP processing and reduces insulin-stimulated lipogenesis. Journal of Clinical Investigation 2004;113:1168-1175.
5. Li Y, Wong K, Walsh K, Gao B, Zang MW. Retinoic Acid Receptor beta Stimulates Hepatic Induction of Fibroblast Growth Factor 21 to Promote Fatty Acid Oxidation and Control Whole-body Energy Homeostasis in Mice. Journal of Biological Chemistry 2013;288:10490-10504.
6. Li Y, Xu SQ, Mihaylova MM, Zheng B, Hou XY, Jiang BB, Park O, Luo ZJ, Lefai E, Shyy JYJ, Gao B, Wierzbicki M, Verbeuren TJ, Shaw RJ, Cohen RA, Zang MW. AMPK Phosphorylates and Inhibits SREBP Activity to Attenuate Hepatic Steatosis and Atherosclerosis in Diet-Induced Insulin-Resistant Mice. Cell Metabolism 2011;13:376-388.
7. Li Y, Xu SQ, Giles A, Nakamura K, Lee JW, Hou XY, Donmez G, Li J, Luo ZJ, Walsh K, Guarente L, Zang MW. Hepatic overexpression of SIRT1 in mice attenuates endoplasmic reticulum stress and insulin resistance in the liver. Faseb Journal 2011;25:1664-1679.
8. Zang MW, Zuccollo A, Hou XY, Nagata D, Walsh K, Herscovitz H, Brecher P, Ruderman NB, Cohen RA. AMP-activated protein kinase is required for the lipid-lowering effect of metformin in insulin-resistant human HepG2 cells. Journal of Biological Chemistry 2004;279:47898-47905.
9. Zang MW, Xu SQ, Maitland-Toolan KA, Zuccollo A, Hou XY, Jiang BB, Wierzbicki M, Verbeuren TJ, Cohen RA. Polyphenols stimulate AMP-activated protein kinase, lower lipids, and inhibit accelerated atherosclerosis in diabetic LDL receptor-deficient mice. Diabetes 2006;55:2180-2191.

10. Zang M, Gong J, Luo L, Zhou J, Xiang X, Huang W, Huang Q, Luo X, Olbrot M, Peng Y, Chen C, Luo Z. Characterization of Ser338 phosphorylation for Raf-1 activation. J Biol Chem 2008;283:31429-31437.
11. Hou X, Xu S, Maitland-Toolan KA, Sato K, Jiang B, Ido Y, Lan F, Walsh K, Wierzbicki M, Verbeuren TJ, Cohen RA, Zang M. SIRT1 regulates hepatocyte lipid metabolism through activating AMP-activated protein kinase. J Biol Chem 2008;283:20015-20026.
12. Ruifrok AC. Quantification of immunohistochemical staining by color translation and automated thresholding. Anal Quant Cytol Histol 1997;19:107-113.
13. Maeda K, Cao HM, Kono K, Gorgun CZ, Furuhashi M, Uysal KT, Cao Q, Atsumi G, Malone H, Krishnan B, Minokoshi Y, Kahn BB, Parker RA, Hotamisligil GS. Adipocyte/macrophage fatty acid binding proteins control integrated metabolic responses in obesity and diabetes. Cell Metabolism 2005;1:107-119.
14. Bence KK, Delibegovic M, Xue B, Gorgun CZ, Hotamisligil GS, Neel BG, Kahn BB. Neuronal PTP1B regulates body weight, adiposity and leptin action. Nature Medicine 2006;12:917-924.
15. Hofmann SM, Zhou L, Perez-Tilve D, Greer T, Grant E, Wancata L, Thomas A, Pfluger PT, Basford JE, Gilham D, Herz J, Tschop MH, Hui DY. Adipocyte LDL receptor-related protein-1 expression modulates postprandial lipid transport and glucose homeostasis in mice. Journal of Clinical Investigation 2007;117:3271-3282.
16. Tang T, Zhang J, Yin J, Staszkiewicz J, Gawronska-Kozak B, Jung DY, Ko HJ, Ong H, Kim JK, Mynatt R, Martin RJ, Keenan M, Gao ZG, Ye JP. Uncoupling of Inflammation and Insulin Resistance by NF-kappa B in Transgenic Mice through Elevated Energy Expenditure. Journal of Biological Chemistry 2010;285:4637-4644.
17. Zang MW, Dong MQ, Pinon DI, Ding XQ, Hadac EM, Li ZJ, Lybrand TP, Miller LJ. Spatial approximation between a photolabile residue in position 13 of secretin and the amino terminus of the secretin receptor. Molecular Pharmacology 2003;63:993-1001.
18. Gesta S, Bezy O, Mori MA, Macotela Y, Lee KY, Kahn CR. Mesodermal developmental gene Tbx15 impairs adipocyte differentiation and mitochondrial respiration. Proceedings of the National Academy of Sciences of the United States of America 2011;108:2771-2776.

Table S1. Quantitative RT-PCR primers

Gene	Species	Forward primers	Reverse primers
FGF21	Mouse	CTGGGGGTCTACCAAGCATA	CACCCAGGATTTGAATGACC
CPT1α	Mouse	CCAGGCTACAGTGGGACATT	GAACTTGCCCATGTCCTTGT
MCAD	Mouse	GATCGCAATGGGTGCTTTTGATAGAA	AGCTGATTGGCAATGTCTCCAGCAAA
ACAT1	Mouse	CCCCATTGATTTTCCACTTG	AGCACAACCACACTGAATGC
HMGCS2	Mouse	ATACCACCAACGCCTGTTATGG	CAATGTCACCACAGACCACCAG
HMGCL	Mouse	ACTACCCAGTCCTGACTCCAA	TAGAGCAGTTCGCGTTCTTCC
BDH1	Mouse	GAAGATGCTGTCCGGCTAAG	CACCACTGGTCTGTTTGCAG
β-actin	Mouse	CCACAGCTGAGAGGGAAATC	AAGGAAGGCTGGAAAAGAGC
UCP1	Mouse	CACCTTCCCGCTGGACACT	CCCTAGGACACCTTTATACCTAATGG
DIO2	Mouse	AGAGTGGAGGCGCATGCT	GGCATCTAGGAGGAAGCTGTTC
Cidea	Mouse	ATCACAACTGGCCTGGTTACG	TACTACCCGGTGTCCATTTCT
Cox7a1	Mouse	CAGCGTCATGGTCAGTCTGT	AGAAAACCGTGTGGCAGAGA
PRDM16	Mouse	CAGCACGGTGAAGCCATTC	GCGTGCATCCGCTTGTG
Adiponectin	Mouse	GTTGCAAGCTCTCCTGTTCC	ATCCAACCTGCACAAGTTCC
Leptin	Mouse	TGAAGGATCCGGAAGTGTTC	TCCAAATGTTCCGGAAAGAG
FGF21	Human	ACCTGGAGATCAGGGAGGAT	GCACAGGAACCTGGATGTCT
CPT1α	Human	GCTTTGGAGACCTGCTTTTG	AGGCACTGGGTTGTGAAGAC
β-actin	Human	GATGAGATTGGCATGGCTTT	GTCACCTTCACCGTTCCAGT

Table S2 Gene expression profile in the liver of WT and SIRT1 LKO mice in the fed or fasted states

Genes	Definition	AB Assay ID #	Fed				Fasted			
			WT (n = 4)		LKO (n = 5)		WT (n = 4)		LKO (n = 7)	
			Mean	SEM	Mean	SEM	Mean	SEM	Mean	SEM
Acacb	ACC2 (acetyl-CoA carboxylase beta)	Mm01204683_m1	1.0000	0.5117	1.3948	0.3598	0.7854	0.1605	0.2748	0.0420
Angpt1	Angiopoietin-1	Mm01129232_m1	1.0000	0.2290	1.4178	0.4986	2.3787	0.3903	1.3176	0.3568
Angpt2	Angiopoietin-2	Mm00545822_m1	1.0000	0.2621	1.0307	0.1019	0.7156	0.1379	1.6696	0.8270
Arg1	Arginase-1	Mm00475988_m1	1.0000	0.2670	0.9790	0.1597	1.4233	0.2435	1.1904	0.2566
Arg2	Arginase-2	Mm00477592_m1	1.3300	0.2810	0.8699	0.2684	0.7740	0.2337	0.7588	0.1808
Atp2a2	SERCA 2 (Sarcoplasmic/endoplasmic reticulum calcium ATPase 2)	Mm01201431_m1	1.0000	0.2704	1.0778	0.1100	1.9577	0.2442	1.3220	0.18769
Atp2a3	SERCA 3 (Sarcoplasmic/endoplasmic reticulum calcium ATPase 3)	Mm00443898_m1	1.0000	0.4660	0.6998	0.1829	0.6585	0.1605	0.7141	0.1315
Cat	Catalase	Mm00437992_m1	1.0000	0.3910	0.5127	0.0309	0.4778	0.0606	0.4242	0.0546
CD3e	CD3	Mm01179194_m1	1.0000	0.8818	0.4703	0.2537	0.8108	0.2463	0.1905	0.0085
Cdh5	VE-cad/cadherin5	Mm00486938_m1	1.0000	0.2946	0.8344	0.1268	0.5950	0.0691	0.4508	0.0292
Cox4i1	Cox 4 (cytochrome c oxidase subunit IV isoform 1)	Mm00438289_g1	1.0000	0.2825	0.5266	0.0688	0.4665	0.0576	0.5237	0.0387
Cpt1a	Cpt1a (carnitine palmitoyltransferase 1a, liver)	Mm00550438_m1	1.0000	0.2640	1.2399	0.1592	2.8582	0.1042	2.2033	0.1471
Crmp1	Drp-1 (collapsin response mediator protein 1)	Mm00514390_m1	0.0000	0.0000	0.0000	0.0000	0.0000	0.0000	0.0000	0.0000
ctgf	Connective tissue growth factor	Mm01192933_g1	1.0000	0.2215	0.8117	0.1994	1.8046	0.4443	2.4001	0.52257
cybb	NOX2 (gp91phox)	Mm01287743_m1	1.0000	0.4454	1.0373	0.2099	0.7960	0.1667	0.5178	0.0421
Edn1	Endothelin 1	Mm00438656_m1	1.0000	0.2456	1.2701	0.1947	2.0998	0.3121	1.4642	0.4324
Fgf1	FGF-1 (a-FGF)	Mm0043806_m1	1.0000	0.2998	1.5380	0.3327	2.8674	0.1196	2.1000	0.2372
Fgf2	FGF-2 (b-FGF)	Mm00433287_m1	1.0000	0.4996	0.4960	0.2211	0.7858	0.2887	0.3407	0.0566
Fgf21	**FGF 21**	**Mm00840165_g1**	**1.0000**	**0.1696**	**0.1692**	**0.0753**	**11.7127**	**2.3898**	**4.8701**	**1.2228**
Flt1	Flt (VEGFR2)	Mm00438980_m1	1.0000	0.2697	0.8372	0.0873	0.7286	0.0711	0.7318	0.0495
Glrx	Glutaredoxin-1	Mm00728386_s1	1.0000	0.1787	0.8447	0.1279	2.3928	0.2937	1.5824	0.1758
Glrx2	Glutaredoxin-2	Mm00469836_m1	1.0000	0.2556	1.0936	0.1320	1.2259	0.1109	1.2093	0.0931
Gpx1	Glutathione Peroxidase 1	Mm00656767_g1	1.0000	0.2409	1.2193	0.1213	1.9959	0.2282	1.1752	0.1589
Gsr	Glutathione reductase	Mm00439151_m1	1.3300	0.3750	1.3707	0.4416	2.5620	0.5022	1.6520	0.3585
Hif1a	HIF1alpha	Mm00468878_m1	1.0000	0.2588	0.8141	0.1414	0.9154	0.0810	0.7386	0.0549

Table S2 Gene expression profile in the liver of WT and SIRT1 LKO mice in the fed or fasted states

Genes	Definition	AB Assay ID #	Fed				Fasted			
			WT (n = 4)		LKO (n = 5)		WT (n = 4)		LKO (n = 7)	
			Mean	SEM	Mean	SEM	Mean	SEM	Mean	SEM
Hmox1	Heme oxygenase-1	Mm00516005_m1	1.0000	0.2603	0.8348	0.1711	0.8178	0.1612	1.0266	0.1879
Hras1	H-Ras	Mm00476174_m1	1.0000	0.2789	0.7701	0.1367	0.4860	0.0238	0.5071	0.0530
Icam1	ICAM1	Mm00516023_m1	1.0000	0.3320	2.0389	0.5216	2.0826	0.3839	1.0721	0.0510
Igf1	Insulin like growth factor 1	Mm00439560_m1	1.0000	0.2460	1.5780	0.2497	1.8687	0.1330	0.9627	0.0522
Il18	IL 18	Mm00434225_m1	1.0000	0.3622	1.2349	0.1763	0.5289	0.0848	0.3755	0.0368
Il1b	IL1 beta	Mm01336189_m1	1.0000	0.4104	0.4996	0.0897	0.3316	0.1089	0.3578	0.0585
IL33	IL 33	Mm00505403_m1	1.0000	0.3890	0.8764	0.2169	0.6842	0.0879	0.3317	0.0267
Il4r	Il4 Receptor	Mm00439634_m1	1.0000	0.2218	1.1877	0.1755	1.5164	0.1485	0.9488	0.0969
Il6	Interleukin 6	Mm00446191_m1	1.3300	0.5374	0.4425	0.1985	0.2923	0.1148	0.6028	0.1417
Kdr	Flk-1	Mm00440111_m1	1.0000	0.2575	0.7166	0.1041	0.6135	0.0815	0.5912	0.0366
Keap1	Keap1 (kelch-like ECH-associated protein 1)	Mm00497268_m1	1.0000	0.2742	0.6221	0.0916	0.4285	0.0319	0.6287	0.0650
LIgl1/Mgl1	Macrophage galactose lectin	Mm00839416_m1	1.0000	0.3641	1.0118	0.4457	0.7495	0.1142	1.5269	0.7431
Mcp1	Monocyte chemotactic protein 1	Mm00441242_m1	1.0000	0.6410	0.8619	0.2021	0.2270	0.0899	0.2177	0.0985
Mfn1	Mitofusin 1	Mm00612599_m1	1.0000	0.2512	1.3021	0.1529	1.5877	0.0603	1.0406	0.0830
Mfn2	Mitofusin 2	Mm00500120_m1	1.0000	0.2749	0.8954	0.1207	1.0762	0.0588	0.8386	0.0830
Mip1a	Macrophage inflammatory protein 1a	Mm00441259_g1	1.3300	0.5578	0.6566	0.2047	0.8504	0.1922	0.7047	0.1917
MMP19	MMp19	Mm00491300_m1	1.0000	0.2950	1.7328	0.2234	1.6701	0.2319	1.3121	0.1588
mmp2	MMP2	Mm00439498_m1	1.0000	0.2790	0.7600	0.2063	0.4622	0.0672	0.7735	0.1539
Mmp9	MMP9	Mm00442991_m1	1.0000	0.3522	0.4628	0.1160	0.2910	0.0993	0.3804	0.0812
Ncf1	P47phox	Mm00447921_m1	1.0000	0.5729	2.2559	0.2873	2.0047	0.2231	1.0705	0.2517
Nos3	NOS3 (eNOS)	Mm00435217_m1	1.0000	0.5343	0.6085	0.1247	1.1143	0.1564	1.3341	0.2486
Nox4	NOX 4	Mm00479246_m1	1.0000	0.4836	0.7746	0.2557	0.1860	0.1121	0.6163	0.1978
nrf2	NRF-2	Mm00477784_m1	1.0000	0.2599	0.9895	0.1457	0.6496	0.0847	0.5163	0.0462
Pecam1	PECAM	Mm01242584_m1	1.0000	0.3152	1.1876	0.1714	1.3326	0.1450	1.1502	0.1091
Pparg	PPAR Gamma	Mm01184322_m1	1.0000	0.3099	1.1401	0.1728	1.9204	0.2300	0.7253	0.1921

Table S2 Gene expression profile in the liver of WT and SIRT1 LKO mice in the fed or fasted states

Genes	Definition	AB Assay ID #	Fed				Fasted			
			WT (n = 4)		LKO (n = 5)		WT (n = 4)		LKO (n = 7)	
			Mean	SEM	Mean	SEM	Mean	SEM	Mean	SEM
Ppargc1a	peroxisome proliferative activated receptor, gamma, coactivator 1 alpha	Mm01208835_m1	1.0000	0.3709	0.7149	0.1216	1.7404	0.3575	1.0149	0.2214
Prdx1	Peroxiredoxin 1	Mm01621996_s1	1.0000	0.1192	0.7690	0.1615	0.6356	0.0897	0.8471	0.0816
Prdx2	Peroxiredoxin 2	Mm00448996_m1	1.0000	0.3051	1.3354	0.1868	1.3023	0.1204	1.0232	0.1556
Prkaa2	AMPKa2 (protein kinase, AMP-activated, alpha 2 catalytic subunit)	Mm01264789_m1	1.0000	0.2720	1.1832	0.2194	0.6857	0.0283	0.6936	0.0716
Pten	PTEN	Mm00477210_m1	1.0000	0.2844	1.0477	0.0770	1.7122	0.1402	1.0341	0.0934
Saa1	Saa1	Mm00656927_g1	1.0000	0.5075	1.3438	0.5165	0.8935	0.6454	1.2437	0.8670
Sesn2	Sestrin2	Mm00460679_m1	1.0000	0.7513	0.2567	0.0650	0.8680	0.1318	0.4010	0.0716
Sirt1	Sirt 1	Mm00490758_m1	1.0000	0.4092	0.2159	0.0471	1.4393	0.0605	0.2240	0.0275
Sirt3	Sirt 3	Mm00452129_m1	1.0000	0.2944	1.6288	0.2655	1.4374	0.1119	1.3337	0.1502
Slc2a2	GLUT2 (solute carrier family 2 (facilitated glucose transporter), member 2)	Mm00446229_m1	1.0000	0.3220	0.9282	0.1579	0.7685	0.0891	0.4633	0.0674
Sod1	CuZnSOD (SOD1)	Mm01344233_g1	1.0000	0.2560	0.6467	0.0740	0.5695	0.0907	0.5345	0.0425
Sod2	MnSOD (SOD2)	Mm00449726_m1	1.0000	0.2787	0.9394	0.1206	1.1511	0.0807	0.8085	0.0549
Sod3	ecSOD (SOD3)	Mm01213380_s1	1.0000	0.5314	0.5825	0.1995	0.5923	0.1841	1.1623	0.2100
SPHK1	Sphingosine kinase 1	Mm00448841_g1	1.0000	0.9171	0.2371	0.1526	0.1973	0.1064	0.5016	0.1450
stat3	Signal Transducer and Activator of Transcription 3	Mm01219775_m1	1.0000	0.2727	0.8284	0.1520	0.6417	0.0636	0.5640	0.0375
Tfam	Mitochondrial Transcription factor A	Mm00447485_m1	1.0000	0.2309	1.1577	0.1679	1.2896	0.1122	0.7700	0.0633
Timp2	TIMP2	Mm00441825_m1	1.0000	0.2987	0.4112	0.0909	0.5110	0.0772	0.5483	0.0473
Tlr2	Toll-like receptor 2	Mm00442346_m1	1.0000	0.5849	0.7702	0.1966	0.6207	0.1367	0.3315	0.0768
Tlr4	Toll-like receptor 4	Mm00445273_m1	1.0000	0.3537	1.3637	0.3313	1.3749	0.3503	1.1109	0.1783
tnf	TNFa	Mm00443258_m1	1.0000	0.6672	0.6038	0.1246	0.3754	0.1505	0.1895	0.0371
traf6	Traf6	Mm00493836_m1	1.0000	0.2679	0.9540	0.2180	1.0494	0.0656	0.7193	0.0915
TSP-1/Thbs1	Thrombospondin-1	Mm01335418_m1	1.0000	0.7880	0.2388	0.0872	0.1471	0.0150	0.2598	0.1877
Txn1	Thioredoxin-1	Mm00726847_s1	1.0000	0.3675	0.4339	0.1156	0.4704	0.1704	1.1259	0.1979
Ucp2	UCP2	Mm00627598_m1	1.0000	0.3502	1.0747	0.2100	2.2272	0.2312	1.3722	0.1322
PPARα	PPARalpha	Mm00440939_m1	1.0000	0.3614	1.3762	0.2961	1.9633	0.1783	2.2963	0.3649

Table S2 Gene expression profile in the liver of WT and SIRT1 LKO mice in the fed or fasted states

Genes	Definition	AB Assay ID #	Fed				Fasted			
			WT (n = 4)		LKO (n = 5)		WT (n = 4)		LKO (n = 7)	
			Mean	SEM	Mean	SEM	Mean	SEM	Mean	SEM
Vcam1	VCAM1 (CD106)	Mm01320970_m1	1.0000	0.3666	1.1314	0.1918	1.9640	0.3449	1.6713	0.2136
Vegfa	VEGF A	Mm01281449_m1	1.0000	0.2601	0.8977	0.0763	0.6418	0.0560	0.5183	0.0278
vegfc	VEGF C	Mm00437310_m1	1.0000	0.3998	1.4047	0.2579	1.2690	0.3027	0.6408	0.1590
Vegfa	VEGF A	Mm01281449_m1	1.0000	0.2601	0.8977	0.0763	0.6418	0.0560	0.5183	0.0278
vegfc	VEGF C	Mm00437310_m1	1.0000	0.3998	1.4047	0.2579	1.2690	0.3027	0.6408	0.1590